Manufacturing Technologies and Applications
MATECA

Nano Boron Nitride and Carbon Nanotube in Sensors: Comparative Investigation with ANN

Kübra Keser[1,*], Zafer Kaya[2]

[1]*Department of Electrical and Electronics Engineering, Simav Technology Faculty, Kutahya Dumlupınar University, Kutahya, Türkiye*
[2] *Kutahya Dumlupınar University, Simav Vocational School, Kutahya*

ABSTRACT

Carbon nanotube (CNT) and nanosized boron nitride (BN) materials are widely used support elements in sensor development due to their compatibility and structural versatility. Studies examining physical parameters in such a detailed comparison with ANN are rarely encountered in the literature. The presented study prepared sensors with different amounts of nanomaterials, water, glycerol and gelatin content. The created sensors' glossiness (20°-60°), colour change (ΔE) and hardness parameters were measured. The measurement data were evaluated using statistical methods and the Multilayer Perceptron (MLP) artificial neural network model. Tansig was used as the transfer function, and the mean square error was used as the performance function. The best classification for training and test success was made in the hardness parameter with 99.9% accuracy, followed by ΔE with 94.9% accuracy. ΔE and glossiness were the most effective common structural materials for the experiments with 6 ml of water at 60° test conditions and 9 ml of water for glossiness at 20° and hardness. For ΔE, 0.12 g BN and 0.06 g CNT and for 60° gloss, 0.06 g for both BN and CNT provided the most significant effect on the changes. The experimental conditions of 0.06 g for BN and CNT were also the most influential parameters for the hardness change.

Keywords: *Sensor, BN, CNT, MLP, ΔE, Glossiness*

Sensörlerde Nano Bor Nitrür ve Karbon Nanotüp: YSA ile Karşılaştırmalı İnceleme

ÖZET

Karbon nanotüp (CNT) ve nano boyutlu bor nitrür (BN) malzemeler, uyumlulukları ve yapısal çok yönlülükleri nedeniyle sensör geliştirmede yaygın olarak kullanılan destek elemanlarıdır. Literatürde YSA ile fiziksel parametrelerin bu kadar detaylı bir şekilde karşılaştırılarak incelendiği çalışmalara nadiren rastlanmaktadır. Sunulan çalışmada farklı miktarlarda nanomalzemeler, su, gliserol ve jelatin içerikli sensörler hazırlanmıştır. Oluşturulan sensörlerin parlaklık (20°-60°), renk değişimi (ΔE) ve sertlik parametreleri ölçülmüştür. Ölçüm verileri hem istatistiksel yöntemler hem de Çok Katmanlı Algılayıcı (MLP) yapay sinir ağı modeli kullanılarak değerlendirilmiştir. Transfer fonksiyonu olarak Tansig ve performans fonksiyonu olarak ortalama kare hata kullanılmıştır. Hem eğitim hem de test başarısı için en iyi sınıflandırma %99,9 doğrulukla sertlik parametresinde yapılmış, bunu %94,9 doğrulukla ΔE takip etmiştir. ΔE ve parlaklık, 60° test koşullarında 6 ml su ile, 20°'de parlaklık ve sertlik için de 9 ml su ile yapılan deneylerde en etkili ortak yapısal malzemeler olmuştur. ΔE için 0,12 g BN ve 0,06 g CNT ve 60° parlaklık için hem BN hem de CNT için 0,06 g değişimler üzerinde en büyük etkiyi sağlamıştır. Hem BN hem de CNT için 0,06 g'lık deneysel koşullar da sertlik değişimi için en etkili parametreler olmuştur.

Anahtar Kelimeler*: Sensör, BN, CNT, MLP, ΔE, Parlaklık*

1. INTRODUCTION

CNTs and BN, as important nanotechnology materials, are widely used in biosensors, electronic devices, manufacturing operations, and medical applications [1–7]. Among nanomaterials, CNTs are formed by rolling a graphene sheet to form cylindrical structures at the nanometer scale [8–10]. Carbon nanotubes have good mechanical properties, a large surface area, a fast electron transfer rate and a high melting point [11–14]. In addition, due to their superior properties, such as good biocompatibility, high thermal and electrical conductivity and chemical stability, are considered ideal materials for biosensors and medical devices. BN is

*Corresponding author, e-mail: kubra.keser@dpu.edu.tr

Received 25.04.2025; Revised 12.08.2025; Accepted 01.09.2025
https://doi.org/10.52795/ mateca.1683835
To cite this article: K. Keser, Z. Kaya, Nano Boron Nitride and Carbon Nanotube in Sensors: Comparative Investigation with ANN, Manufacturing Technologies and Applications 6(3) (2025) 248-262.

similar to carbon allotropes in its crystallographic and electronic structure and stands out among artificial compounds. While there are many forms of boron nitride, the most common stable form is hexagonal boron nitride (h-BN). Hexagonal boron nitride (hBN) differs from graphite in its electrical insulation, high thermal shock resistance, and stability at high temperatures. These properties make hBN ideal for use in various industrial fields such as automotive, metal industry, cosmetics and medicine [15,16]. h-BN is a two-dimensional nanostructure consisting of layers held together by Van der Waals interactions, formed by the covalent bonding of boron and nitrogen atoms in a hexagonal arrangement. In addition to its good mechanical properties, structural stability and biocompatibility, h-BN exhibits superior properties such as chemical inertness, high thermal conductivity, low thermal expansion and high electrical resistance, and is also notable for its non-toxicity [17–20].

Gelatin, which is used in producing environmentally friendly, biodegradable sensors, is one of the most promising biopolymers with features such as renewable, low price, and easy processability [21]. When biosensors are evaluated in terms of production techniques, some processing techniques, such as surface activation, modification, in situ polymerisation, etc., are laborious and expensive, involve complex processing steps and are generally challenging for industrial applications. Therefore, to obtain the best result in terms of cost-benefit, easy processing methods should be determined. The solution casting technique is a highly efficient and cost-effective way [22,23].

One of the most interesting areas of carbon nanotube use is biopolymer biosensors, which include chemical and biological sensing applications [24]. These are electrochemical sensors, optical sensors and field effect devices. Biosensors are sensors consisting of a bioreceptor and a transducer, in their simplest definition. The most basic features sought in a biosensor are repeatability, stability, scalability, simplicity, and cheapness [25]. The material properties and production methods used to produce biosensors affect these properties. Creating and producing biosensors is difficult because it requires complex processing techniques such as surface activation, modification, immobilisation, and transduction steps. One of the desired properties of biosensors is glossiness. Although it varies according to the intended use of the biosensor, it is preferred that the sensor surface is not too bright so that the glossiness does not cause measurement errors in bio-recognition processes, analyte detection and in cases where the results need to be visually evaluated and interpreted. The film structures used as sensors should be as flexible as possible to expand the use field and ease of use. Therefore, the hardness of the films formed must be measured.

In nano biosensors, physical, chemical and biological properties increase in addition to biocompatibility, and sensors can be easily functionalized [13,25]. Biocompatibility refers to the interoperability of sensors with biological components such as enzymes, DNA, and antibodies [13]. Carbon nanotubes are also very effective in creating support structures for these sensors [25]. Alam et al. [22] obtained nanocomposites by creating a solution in which the ratio of gelatin to glycerol was kept at 3:1 and adding single-walled carbon nanotubes to this mixture at different ratios. They determined a possible interaction between the –OH group of water and glycerol in the single-walled carbon nanotube solution and the NH_2^- groups of gelatins. It was found that the film's roughness increased due to the formation of the interface bond between the carbon nanotube and the polymer matrix, along with the increase in the concentration of the single-walled carbon nanotube filler. Alam et al., in another study [21], investigated the electrical conduction properties of the composite structure formed by adding a multi-walled carbon nanotube aqueous solution, a small amount of gelatin solution and glycerol as a plasticiser.

Hexagonal boron nitride (h-BN), which has the same lattice structure as graphene, has similar properties to graphene, such as muscular mechanical strength and good adsorption performance [12,13,25]. In addition to these properties, it also has superior properties to graphene, such as oxidation resistance, electrical insulation, and wide energy gap band [21,26,27]. In addition, they play an active role in biomedical applications with their properties, such as good biocompatibility, high chemical and mechanical stability, high elastic modulus, and biodegradability [26].

Lima et al. [20] have used boron nitride-based nanocomposites in different applications by mixing the aqueous dispersion of boron nitride nanoparticles with monomers or polymeric chains dissolved in water or, in some cases, in ethanol. Good distribution of boron nitride in the hydrogel matrix dramatically improves the mechanical properties by effectively increasing the load transfer. In addition, boron nitride can be used as a filler material in hydrogels to increase biocompatibility and improve mechanical properties. It has also been reported that nanoparticle-doped hydrogels enhance mechanical strength and Young's modulus and are also used in drug delivery applications, intelligent systems and water treatment. Li et al. [28] performed molecular dynamics simulations to systematically investigate the mechanical and thermal properties of carbon nanotubes and boron nitrides. It was found that carbon nanotubes have a higher elasticity modulus, and their thermal conductivity varies with different temperature changes.

Algharagholy et al., which examines the effects of CNT and BN layers on sensor behaviour via electrical conductivity, provides a detailed model for the sensitivity of molecular binding to conductivity changes and molecular dissociation in the BN region. The analytical modelling focuses on electrical mechanisms and sensitivity rather than our study's physical colour/gloss parameters [29]. The study, which includes thermal and electrical properties of CNT and BN-added rubber polymer composites, EMI shielding with layering approaches, and thermal conductivity, presents physical performance data at wt% levels, including the density and distribution of additives, and nanomechanical effects of composite structures [30]. Another study systematically analyses carbon nanomaterial-filled polymer sensors' physical (stiffness, flexibility) and thermal (temperature sensing) sensitivities. While similar to our study in that it addresses sensor polymers' stiffness, flexibility, and sensing behaviour, this study only includes carbon fillers instead of CNT/BN [31]. One study provides a general overview of sensor applications' physicochemical and mechanical performance involving carbon nanomaterials such as CNTs, graphene, and fullerene. This review article examines sensor functions (communication, environmental sensitivity, and long-term stability) using CNTs and partially evaluates physical parameters [32]. Compares the sensor performance of CNT vs. BN nanotubes concerning different functional groups (–NH_2, –COOH, –NO_2) and evaluates their ion response properties. This study directly compares physical and electrical sensor performance (sodium and potassium ion sensitivity) [33]. In this study, an effective bifunctional electrocatalyst was obtained for both oxygen reduction (ORR) and oxygen evolution reaction (OER) by developing a nanocomposite based on carbon nanotubes (CNTs) and hexagonal boron nitride (h-BN). CNTs and h-BN were synthesized by hydrothermal methods and annealed at 750 °C. TEM, XRD, XPS, and Raman spectroscopy were used for structural and morphological characterisation. Electrochemical performance was evaluated [34]. This study aims to evaluate the progress of carbon nanotube (CNT)-based electrochemical sensors in biological analysis applications. Methods for the synthesis, purification, functionalization, and integration into electrodes of CNTs are reviewed. The application of CNT-based electrochemical sensors for detecting numerous biomolecules, including glucose, neurotransmitters, proteins, DNA, cells, and microorganisms, is examined in detail. CNTs are described as suitable electrode materials due to their high surface area, low overpotential, rapid electron transfer, and resistance to surface fouling. Furthermore, their potential for widespread use in clinical diagnosis, food control, and environmental analysis is highlighted [35]. In recent years, studies on biodegradable sensor technologies have increased the search for environmentally friendly materials and the trend towards sustainable production techniques. For example, Ko et al. (2021) significantly contributed to wearable sensor applications by fabricating solvent-free CNT-doped flexible films [1]. In 2023, Bahrami Miyanji and his team highlighted the potential of CNT-reinforced gelatin-based nanocomposite structures in tissue engineering [36]. Also in 2024, Zhao et al. detailed the effects of CNT-doped carbon fibre composites on surface conductivity and mechanical strength [12]. Studies in the literature that examine the effects of changes in nano-sized BN and CNT additive ratios on the physical properties of the resulting composites using glycerol and gelatin as a binder in biodegradable films in such a detailed and comparative manner using artificial neural networks (ANNs) are rare. As seen in the literature review [21,36–39], there are studies on biopolymer-based sensors containing CNTs and BN additives, but these studies do not include physical parameter-focused ANN modelling. In the studies, it is seen that the focus is generally on material structure, surface morphology, and thermal and mechanical performance [40,41]. This gap exists, particularly in the simultaneous investigation of physical optical parameters with modeling. Filling this gap in the literature will contribute to developing more effective and reliable sensors in industry and biomedical fields. Sensors can be exposed to various external factors in their environments. Sensors must have sufficient rigidity to absorb impacts. Furthermore, when positioned on a flexible material like fabric, they must be able to operate in coordination with this material. Sensors must also possess characteristics that ensure compatibility in terms of color and gloss within the systems in which they are used. The color and gloss characteristics of sensors interact with heat and light sources, causing the data being measured to be erroneous. Furthermore, due to this interaction, the signals transmitted to the sensor or the signals it generates may be interpreted differently than intended. Color and gloss sensitivities directly affect the operating conditions of the systems in which the sensors operate. Firstly, sensors are manufactured by combining different elements. The quantity or size of each of these elements gives the sensor different properties. In addition to functional properties, physical properties also vary depending on these elements. Examining the impact of sensor elements on physical properties has been deemed an important topic. While numerous studies have focused on the functional properties of sensors, the fact that their physical properties have been studied less has motivated this study. This study is one of the first comprehensive comparative studies to analyze the physical properties (gloss, ΔE, and hardness) of CNT- and BN-doped biodegradable sensors using ANN (MLP). The literature typically examines functional properties such as electrical conductivity and thermal stability. However, physical parameters such as ΔE, gloss, and hardness are crucial

for visual perception and sensor performance under application conditions. Furthermore, simultaneous measurement and modeling of these three physical parameters with an ANN fills a gap in the literature. In the presented study, it is aimed to reveal the potential of CNT and BN by ANN methods to improve the performance of materials used in sensor production. For this purpose, the surface morphology of biodegradable films formed by using different ratios of nano additives, glycerol and gelatin will be investigated experimentally. Then, the data obtained from the experiments for each parameter will be evaluated comparatively with ANN.

2. MATERIAL AND METHOD

2.1. Materials

Commercial colourless gelatin (Bovine gelatin, Dr. Oetker (% 100%)- 2408155), glycerol (Glycerin-Health (% 80%)- GL139), purified water-deionised water (DIW), EN/MWCNT703 (10-20 μm - Ege Nanotek (% 95%)), BN (BORTEK Bor Technologies and Mechatronics Industry and tic. Inc. 120 nm-hexagonal structure) purchased samples were used.

2.2. Method

The solution casting technique was used as an easy-to-produce, simple, cheap and highly efficient method for an environmentally friendly, biodegradable and biocompatible sensor structure [22]. Since the starting point of this study was to examine the effects of the changing concentration amount and various nanomaterials on the sensors' physical properties, a suitable preparation plan was made for this purpose. The amounts and levels of additives that make up the produced sensors are shown in Table 1.

Table 1. Parameters used in sensor preparation

Parameters	Level 1	Level 2	Level 3
Water (ml)	3	6	9
Gelatin (g)	0.15	0.30	0.45
Glycerol (g)	0.075	0.15	0.225
BN / CNT (g)	0.06	0.12	0.18

The Taguchi method was used as the experimental design and analysis method. Here, the steps of determining the factors and interactions, determining the levels of each factor, selecting the appropriate orthogonal matrix, transferring the factors and interactions to the columns of the orthogonal matrices, performing the experiments, analysing the data, determining the optimal levels, and performing the verification experiments were carried out. Fifty-four experiments were carried out for BN and CNT-doped sensors with the L27 orthogonal experimental design (Table 2).

In preparing the sensors, gelatin and glycerol, preferred as a plasticiser, were dissolved in pure water at room temperature in the amounts specified in the experimental parameters. Afterwards, CNT and BN solutions were mixed separately and homogeneously. The formed solutions were poured onto transparent plates with dimensions of 129×45×19 mm for sensor formation. These samples were left to dry for 8 hours in open air flow at room temperature and separated from the transparent plates. The measurement process began after the films were created. The stages of the study are shown in Figure 1.

In the glossiness meter that can measure at 20°, 60°, and 85°, 20° measurements are used to identify glossiness surfaces, 85° measurements are used to identify matte surfaces, and 60° measurements are used to identify both matte and glossiness surfaces [42]. In the study, the glossiness measurements of the sensors were carried out at 20° and 60° with the MicroTRI-gloss μ (Glossmeter) (BYK Gardner brand, TS4318 EN ISO 2813-2014) glossiness measurement device. 20° measurements were considered to define how bright the sensors produced were, and 60° measurements were supposed to represent how close they were to matte. Glossiness measurements were performed in triplicate, and the results were evaluated by calculating their means and standard deviations.

Table 2. Experimental design created with L27 Orthogonal array

Experiment no	Water (ml)	Gelatin (g)	Glycerol (g)	Coating amount (g)
1	3	0.15	0.075	0.06
2	3	0.15	0.075	0.06
3	3	0.15	0.075	0.06
4	3	0.30	0.150	0.12
5	3	0.30	0.150	0.12
6	3	0.30	0.150	0.12
7	3	0.45	0.225	0.18
8	3	0.45	0.225	0.18
9	3	0.45	0.225	0.18
10	6	0.30	0.075	0.18
11	6	0.30	0.075	0.18
12	6	0.30	0.075	0.18
13	6	0.45	0.150	0.06
14	6	0.45	0.150	0.06
15	6	0.45	0.150	0.06
16	6	0.15	0.225	0.12
17	6	0.15	0.225	0.12
18	6	0.15	0.225	0.12
19	9	0.45	0.075	0.12
20	9	0.45	0.075	0.12
21	9	0.45	0.075	0.12
22	9	0.15	0.150	0.18
23	9	0.15	0.150	0.18
24	9	0.15	0.150	0.18
25	9	0.30	0.225	0.06
26	9	0.30	0.225	0.06
27	9	0.30	0.225	0.06

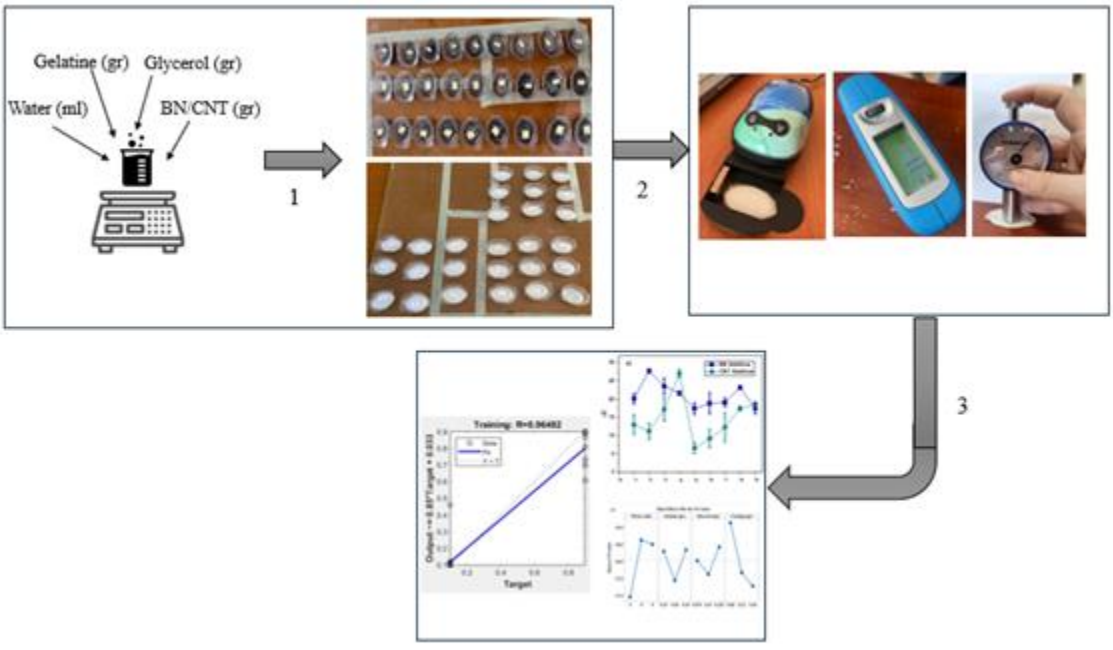

Figure 1. Working steps (1: Production, 2: Measurement, 3: Analysis)

Colour was measured depending on the concentration of CNT and BN-doped sensors prepared at different concentrations. For this purpose, the Colorstriker colour measuring device (ASTM-D2244) was used, which has the measuring feature in the CIE *L*a*b** colour system (Figure 1). The measurements were carried out in triplicate for both doped sensors. In the measurement of *L*, a**, and *b** values, *L**Indicates the color change from black to white (*L** = 0 black, *L** = 100 white). *a**: Defines the colour change from red to green. The tendency towards red is positive; the tendency towards green is negative. This range is defined by the values +127 to -128. *b**: It represents the colour range between yellow and blue. Like the *a** value, this range is

defined by the values +127 to -128 [42–44]. In the colour system, the origin of this system is $a^* = 0$, $b^* = 0$ and $L^* = 50$, representing the actual neutral grey colour [43–46]. ΔE was used to describe the colour properties of the produced sensors with a single concept. The origin of the colour system was taken as a reference in ΔE calculations. The amount of deviation from the origin was found using Equation 1 for each sensor base test sample.

$$\Delta E = \sqrt{(L_1 - L_2)^2 + (a_1 - a_2)^2 + (b_1 - b_2)^2} \quad (1)$$

Here, ΔE defines the amount of color difference. L_1, a_1, and b_1 express the coordinate values of the neutral gray color ($L_1 = 50$, $a_1 = 0$ and $b_1 = 0$), L_2, a_2 and b_2 express the color values of the measured films.

The hardness measurement of the produced sensor structures was carried out with a Shore D hardness measuring device (Tronic brand) (Figure 1). In this device, the measurement is made by inserting needles into the films and measuring the depth of the inserted needle by applying a certain force to determine the relative hardness degree. As with the other parameters, three repeated measurements were performed for each sensor structure, then the average and standard deviation values were calculated.

This study used ANN because modelling complex and multiple parameters, such as ΔE, gloss, and hardness, using classical statistical methods can yield limited results. It allows for more effective modelling of the interactions between parameters by evaluating the effects of parameters individually and collectively in multivariate systems. It also provides flexibility in estimating the effects of different additive ratios and performing optimisations. Furthermore, ANN is used in our study as a tool that complements experimental methods and enables advanced analysis.

The MLP structure, an artificial neural network architecture (Figure 2), was created using the Matlab-nntool interface and the classes created for each parameter are shown in Table 3. Since the effects of the selected parameters on different outputs will be observed, classes specific to each production were created to make the classification more accurate and precise. In this neural network, 67% of the dataset was used for training, while 33% was used for testing (data was selected randomly). The Levenberg-Marquardt (Train LM) adaptation learning function was used to classify and model the MLP structure with five neuron input layers. The TrainLM algorithm was chosen because it provides the fastest convergence for small neural network models operating with small datasets and minimizes the error function efficiently. It is also frequently used for classification models with small datasets in the MATLAB environment. Tansig was defined as the transfer function, and the mean square error was determined as the performance function. The epoch number was determined as 1000, and the early stopping method and 33% test data separation were applied to prevent overfitting. Loss function curves and validation error analyses have been added.

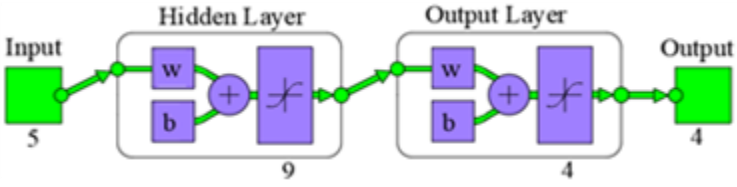

Figure 2. MLP network architecture

Data for ΔE, gloss, and hardness values were divided into four classes. When creating classes, the clustering intervals were chosen to be equally sized and consistent with the natural distribution, considering the existing data distribution. For example, for ΔE, the observed values between 6.6 and 28.1 were divided into four equally spaced classes. This classification enabled a more balanced class sampling in the ANN model and strengthened class distinguishing features (Table 3).

Table 3. Classes of parameters

	Class I	**Class II**	**Class III**	**Class IV**
ΔE	6.6-11.9	12-17.3	17.4-22.7	22.8-28.1
Glossiness 20°	0.2-0.575	0.576-0.95	0.96-1.326	1.327-1.71
Glossiness 60°	0.9-3.37	3.38-5.84	5.85-8.31	8.32-10.78
Hardness (Shore D)	6.33-11.915	11.92-17.5	17.6-23.09	23.1-28.68

In the last stage, the Taguchi optimisation method was used to obtain the optimum results for each value. These results can sometimes be any of the existing experiments, and sometimes they can be the result of an experiment other than the experiments performed. Therefore, verification experiments, which are a method that can be used in these cases, were performed.

2.3. Advantages and Limitations of the Methods Used

The Taguchi method used in this study is a low-cost and time-saving method that allows for systematically analysing the effects of parameters without the need for numerous experiments. Using the L27 orthogonal design, optimal combinations were determined for three levels of each of the four parameters. However, the Taguchi method only evaluates the main effects, revealing limited interactions between parameters; this neural network requires additional modelling in complex systems. Therefore, the Multilayer Perceptron (MLP) artificial neural network model was used in this study. MLP stands out for its ability to process different input variables (numerical/measured) and learn complex and nonlinear relationships. The Levenberg–Marquardt algorithm achieved high accuracy with a low epoch count. However, when the data set is small, there may be a risk of overfitting. This study used test data separation (33%) and early stopping to mitigate this risk. In the future, the model's generalisation ability can be improved with larger data sets.

3. EXPERIMENT AND OPTIMIZATION RESULTS

Each parameter was measured separately for all sensors. The averages of the measurement results were calculated, and these values are shown in Table 4 and 5. In order to evaluate the data obtained from the hardness, glossiness and ΔE data measurements of the samples, graphs were drawn in the OriginPro 2018 program.

Table 4. Physical properties of BN-based sensor substrates obtained from measurements

Exp. no	Water (ml)	Gelatin (g)	Glycerol (g)	Coating amount (g) (BN)	BN			
					ΔE	Glossiness (20°)	Glossiness (60°)	Hardness (Shore D)
1	3	0.15	0.075	0.06	18.52	2.3	20.6	8
2	3	0.15	0.075	0.06	17.80	1.4	8.7	11
3	3	0.15	0.075	0.06	24.07	1	3	4
4	3	0.30	0.150	0.12	28.17	1.1	2.1	4
5	3	0.30	0.150	0.12	26.20	1.2	2.9	10
6	3	0.30	0.150	0.12	28.82	0.6	2	5
7	3	0.45	0.225	0.18	17.88	1.1	1	35
8	3	0.45	0.225	0.18	28.26	1.1	0.3	12
9	3	0.45	0.225	0.18	24.44	1.2	1.4	12
10	6	0.30	0.075	0.18	20.80	1.2	1.8	8
11	6	0.30	0.075	0.18	23.42	1.1	1.8	12
12	6	0.30	0.075	0.18	20.89	0.9	2.2	30
13	6	0.45	0.150	0.06	14.29	2.8	3.8	20
14	6	0.45	0.150	0.06	16.43	1.2	13.3	18
15	6	0.45	0.150	0.06	21.52	1.1	4.1	22
16	6	0.15	0.225	0.12	23.56	0.5	2.8	13
17	6	0.15	0.225	0.12	10.75	1.2	2.2	7
18	6	0.15	0.225	0.12	22.33	1.1	4.4	20
19	9	0.45	0.075	0.12	19.90	1.2	1.6	32
20	9	0.45	0.075	0.12	15.82	1.2	2.4	40
21	9	0.45	0.075	0.12	21.47	1.3	2	14
22	9	0.15	0.150	0.18	23.42	1.2	1.8	20
23	9	0.15	0.150	0.18	21.84	1.2	1.7	11
24	9	0.15	0.150	0.18	24.35	1.2	1.6	13
25	9	0.30	0.225	0.06	17.98	1.2	2.6	14
26	9	0.30	0.225	0.06	20.89	1.1	2.1	17
27	9	0.30	0.225	0.06	13.58	1.2	4.7	15

Table 5. Physical properties of CNT-based sensor substrates obtained from measurements

Exp. no	Water (ml)	Gelatin (g)	Glycerol (g)	Coating amount (g) (CNT)	CNT			
					ΔE	Glossiness (20°)	Glossiness (60°)	Hardness (Shore D)
1	3	0.15	0.075	0.06	28.24	0.5	2.8	18
2	3	0.15	0.075	0.06	5.32	1.2	4.8	18
3	3	0.15	0.075	0.06	17.42	2	7.3	22
4	3	0.30	0.150	0.12	16.36	0.2	1	16
5	3	0.30	0.150	0.12	11.44	0.3	1.2	13
6	3	0.30	0.150	0.12	5.88	0.7	3.4	20
7	3	0.45	0.225	0.18	8.35	0.9	4.9	23
8	3	0.45	0.225	0.18	22.95	0.2	2.1	11
9	3	0.45	0.225	0.18	20.41	0.1	0.8	21
10	6	0.30	0.075	0.18	28.77	0.2	2.2	21
11	6	0.30	0.075	0.18	23.72	0.2	0.8	15
12	6	0.30	0.075	0.18	28.62	0.2	1.1	30
13	6	0.45	0.150	0.06	10.72	0.6	3	24
14	6	0.45	0.150	0.06	5.29	0.5	1.6	20
15	6	0.45	0.150	0.06	3.74	0.8	3.3	23
16	6	0.15	0.225	0.12	11.24	0.4	1.4	16
17	6	0.15	0.225	0.12	14.24	0.7	0.2	16
18	6	0.15	0.225	0.12	2.20	0.9	2.8	21
19	9	0.45	0.075	0.12	21.97	0.8	2.2	10
20	9	0.45	0.075	0.12	12.73	0.6	1.9	28
21	9	0.45	0.075	0.12	2.13	1.7	8.4	19
22	9	0.15	0.150	0.18	19.02	0.9	2.4	21
23	9	0.15	0.150	0.18	17.08	0.7	2.4	21
24	9	0.15	0.150	0.18	16.14	3.1	7.1	19
25	9	0.30	0.225	0.06	19.08	0.5	1.6	8
26	9	0.30	0.225	0.06	16.33	0.7	1.1	14
27	9	0.30	0.225	0.06	20.13	1.1	2.4	28

In general, sensors with BN additives show higher values. However, except for studies where colour change in sensors needs to be monitored (such as colourimetric sensor structures), it is desired to have no or very little colour change. When evaluating concentration-dependent colour change values, choosing the fifth experimental group with CNT additives would be more accurate since the colour change is minimal (Figure 3).

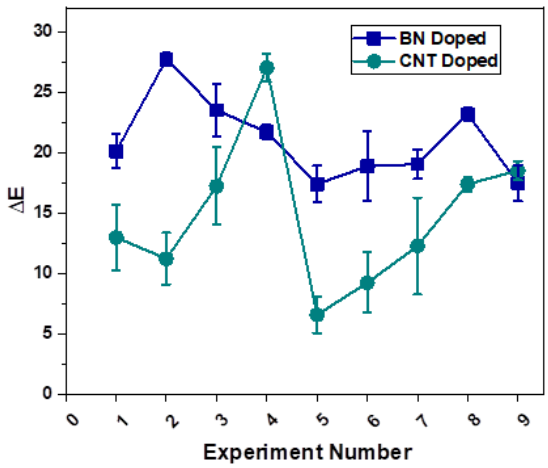

Figure 3. *ΔE* change

Parameters such as the purpose of the sensors and the experimental environment in which they will be used are effective in selecting glossy or matte. The glossiness of the sensors can be clearly distinguished in the 20° graph, and the glossiness is higher in BN-doped sensors. In order to create a glossy sensor structure, it is better to examine the graph in Figure 4 and select the fifth experimental group with BN doping, which has higher glossiness.

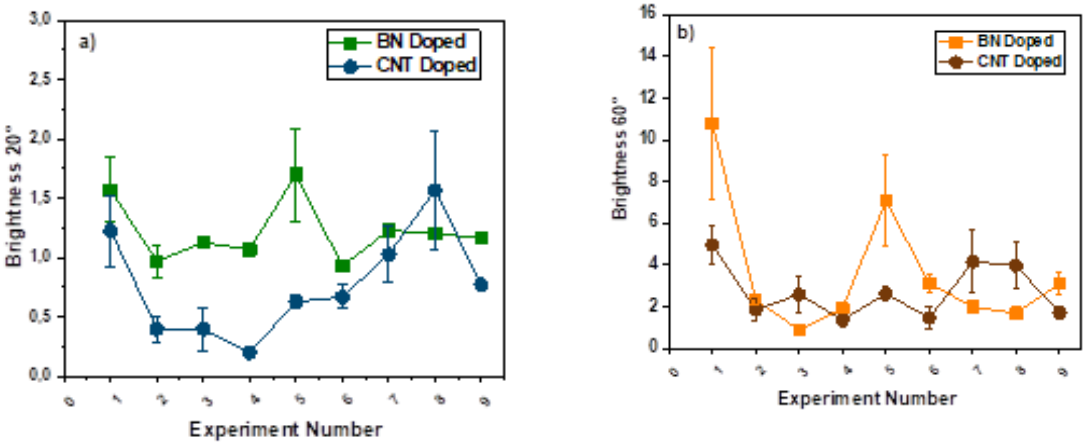

Figure 4. Glossiness change a) 20° b) 60°

When Figure 5 is examined, it is seen that the hardness value of CNT-doped sensors is generally higher. Since neither a hard nor a soft structure is desired in the sensor architecture, choosing CNT-doped sensors with an average hardness value would be more accurate.

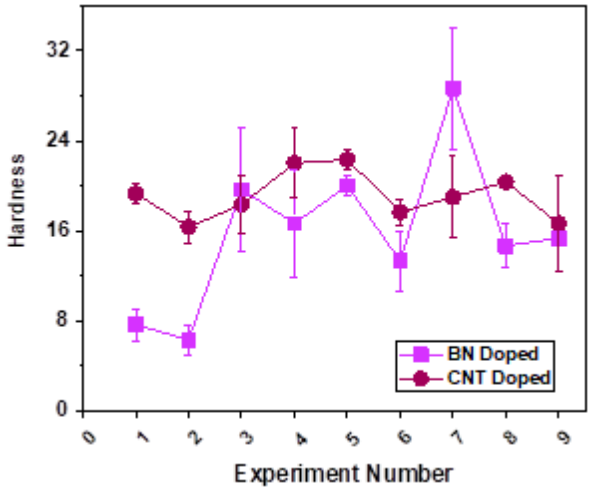

Figure 5. Hardness change

When the effects of sensor components on the ΔE on the classification success rate are interpreted using MLP results obtained using 54 data sets separately for each parameter, it is seen that the classification accuracy rates are pretty high when examining the gloss and hardness parameters (Figure 6). When examined according to the correlation coefficient, it is revealed that each parameter can be easily classified and distinguished with accuracies of 95%, 88.3%, 84%, and 99.9%, respectively. It is observed that the amount of change in each component allows for a clear distinction between the examined parameters. High accuracy values were obtained, particularly for the hardness parameter. This is primarily due to the hardness parameter being closer to a linear distribution, resulting in more distinct class separation, a clear separation of the class intervals used in the model, and a balanced training data balance. The model was created with a 67% training-33% test split, and 99.9% accuracy was achieved on test data not included in the training set. This significantly reduced the risk of overfitting. Additionally, early stopping was used.

To determine the optimum parameter for each factor, main effect graphs created using S/N response were given and evaluated separately (Figures 7-10). The best value for any parameter was found according to the most significant S/N ratio obtained among all parameter levels.

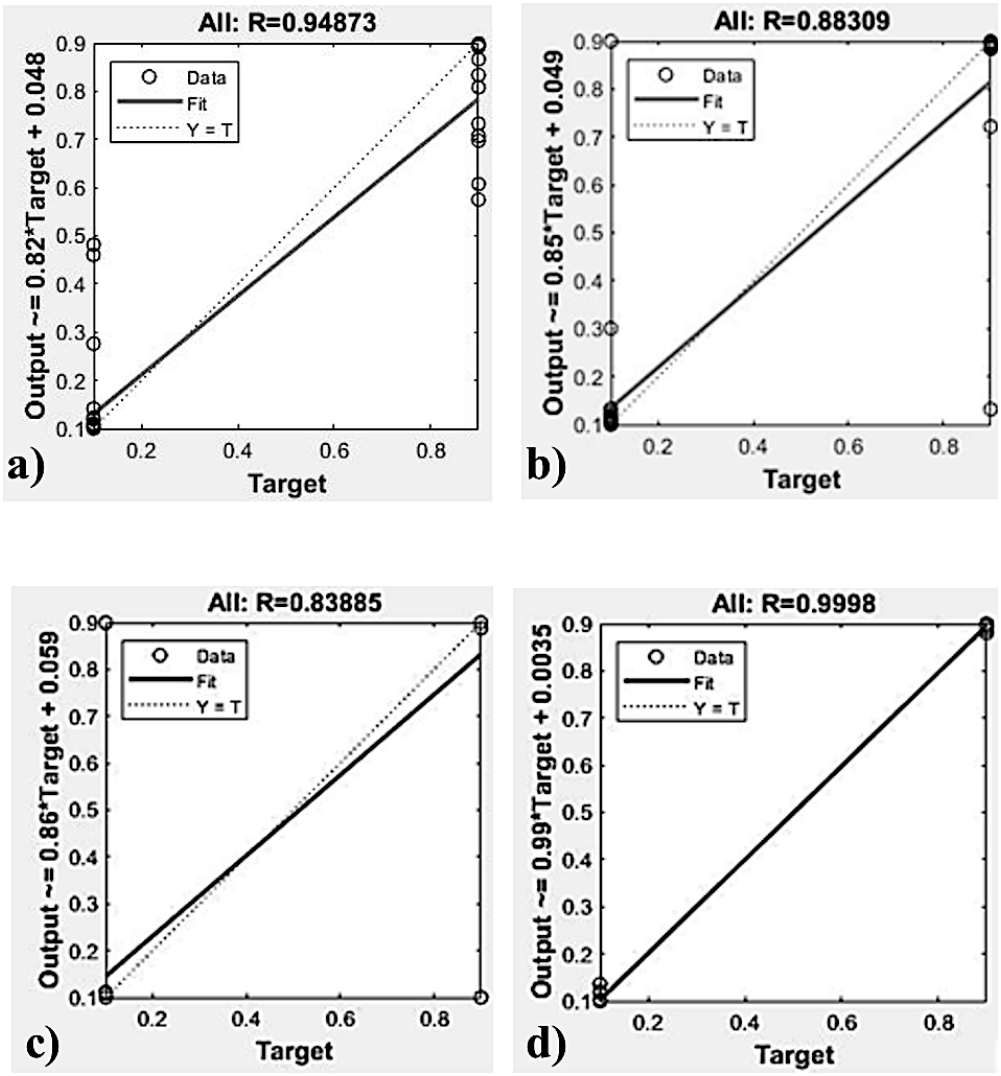

Figure 6. MLP regression plots (a) *ΔE* (b) Glossiness 20° (c) Glossiness 60° (d) Hardness

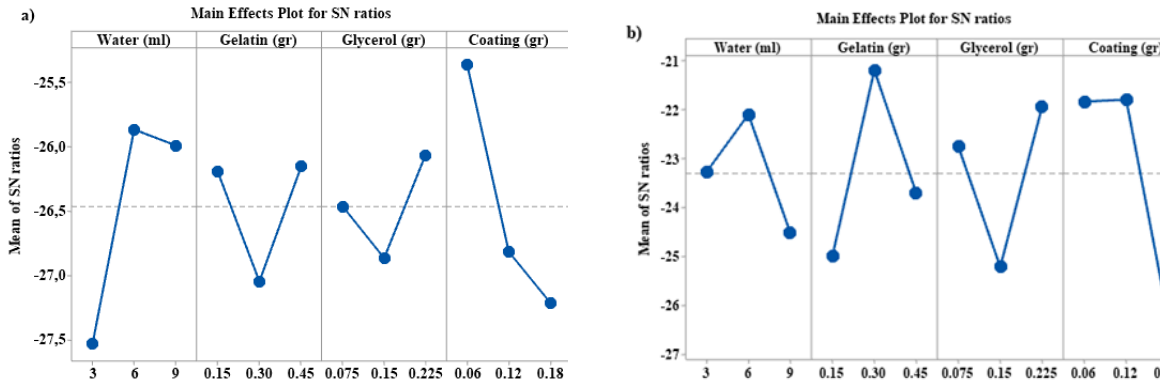

Figure 7. *ΔE* a) BN b) CNT

When the graph is evaluated (Figure 7a-b), it is seen that 6 ml of water, 0.30 g of gelatin, 0.225 g of glycerol, and 0.12 g of coating values are effective parameters for BN-doped sensors. While a decrease in the S/N ratio is observed as the doping amount increases, the S/N ratios are pretty close to each other in cases where the gelatin amount is 0.15 g and 0.45 g. For CNT-doped sensors, these values are 6 mL of water, 0.45 g of gelatin, 0.225 g of glycerol, and 0.06 g of coating, respectively. In these sensors, the S/N ratios are pretty close in cases where the coating amount is 0.06 and 0.12 g.

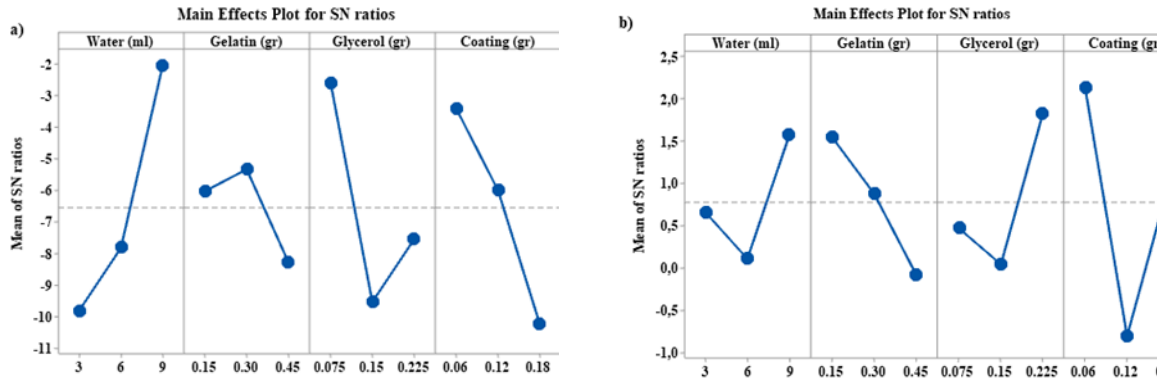

Figure 8. Glossiness 20° a) BN b) CNT

It is seen that 9 ml of water, 0.15 g of gelatin, 0.225 g of glycerol, and 0.06 g of coating values are effective parameters for BN-doped sensors (Figure 8a). In addition, the S/N ratio increased as the amount of water increased, while the S/N ratio decreased as the amount of coating increased. For CNT-doped sensors, 9 ml of water, 0.30 g of gelatin, 0.75 g of glycerol, and 0.06 g of coating are the effective parameters (Figure 8. b). As gelatin increased in these sensors, the S/N ratio decreased.

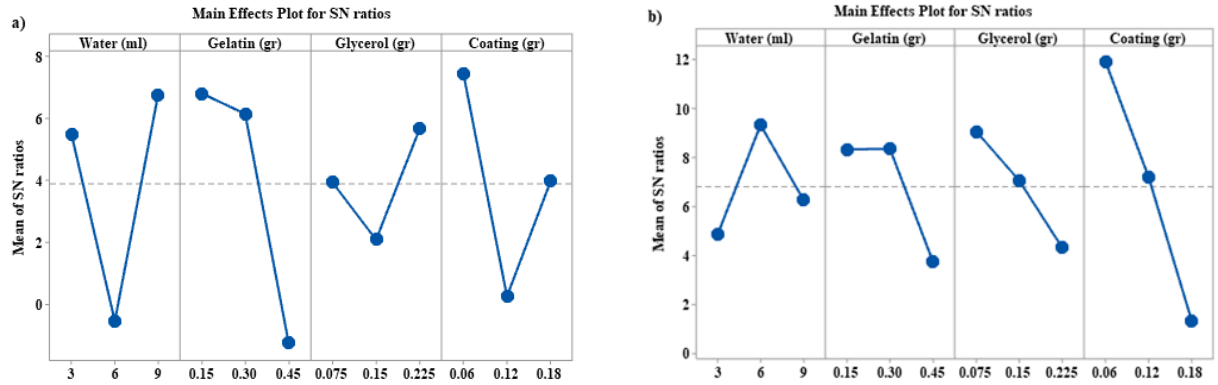

Figure 9. Glossiness 60° a) BN b) CNT

When the graphs in Figure 9 are evaluated, it is interpreted that 6 ml of water, 0.30 g of gelatin, 0.075 g of glycerol, and 0.06 g of coating values are effective parameters for BN-doped sensors. In these sensors, it is seen that the increase in the amount of gelatin causes the S/N ratio to decrease. 9 ml of water, 0.15 g of gelatin, 0.225 g of glycerol, and 0.06 g of coating are effective parameters for CNT-doped sensors. When the amount of gelatin is 0.15 to 0.30 g, the S/N ratio does not change much, but the S/N ratio decreases as the amount of glycerol and the amount of additives increase.

In terms of hardness, when evaluated by looking at the main effect graphs (Figure 10), 9 ml water, 0.30 g gelatin, 0.225 g glycerol, and 0.06 g coating values are effective parameters for BN-doped sensors. For CNT-doped sensors, 9 ml of water, 0.15 g of gelatin, 0.225 g of glycerol, and 0.06 g of coating values are effective, respectively. In these sensors, the S/N ratio increases as the amount of water and glycerol increases, while the S/N ratio decreases as the amount of doping increases.

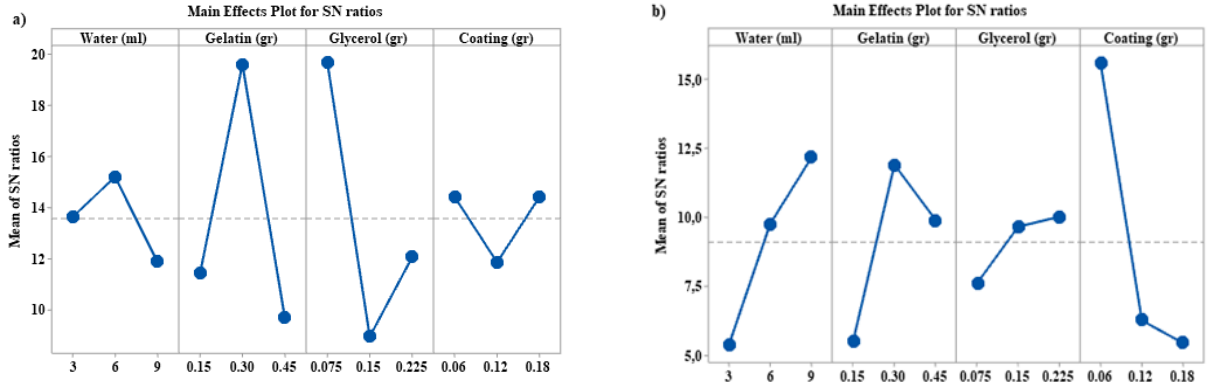

Figure 10. Main effect graphs for Hardness a) BN b) CNT

When we look at the verification experiments, we see that an experiment with optimum results for the hardness parameter was included in the experimental sets. However, the optimum results for *ΔE* and glossiness were obtained under different conditions than the existing experiments. The values obtained from the calculations and verification experiments are presented in Table 6. When we look at the predicted value and validation experiment results, we see that the difference is relatively small, and these results confirm the other stages of the study.

Table 6. Optimum results and validation experiments for parameters

Taguchi Optimization	BN Doped Sensors			CNT Doped Sensors		
	Levels	Predicted Value	Validation Experiment	Levels	Predicted Value	Validation Experiment
ΔE	6 mL 0.30 g 0.225 g 0.12 g	21	25.96	6 mL 0.45 g 0.225 g 0.06 g	22.4	17.7
Glossiness 20°	9 mL 0.15 g 0.225 g 0.06 g	1.66	1.3	9 mL 0.30 g 0.075 g 0.06 g	1.7	1.9
Glossiness 60°	6 mL 0.30 g 0.075 g 0.06 g	9	9.9	9 mL 0.15 g 0.225 g 0.06 g	4.8	5
Hardness	9 mL 0.30 g 0.225 g 0.06 g	20.3	17.5	6 mL 0.30 g 0.075 g 0.18 g	21	22

In this study, the effects of nano-sized BN and CNT additives on gloss, colour difference (*ΔE*), and hardness in biodegradable gelatin-based sensor structures were analysed in detail. The measured parameters were evaluated using traditional statistical methods and a multilayer artificial neural network (MLP) model. In the classification analysis conducted with ANN, the highest accuracy was obtained for the hardness parameter (99.9%), followed by *ΔE* (95%), gloss at 20° (88.3%), and 60° (84%). These results demonstrate that ANN modelling has a strong discrimination ability on physical parameters. Based on the experimental findings, less colour change was observed in CNT-added samples, demonstrating the advantage of CNTs in applications where visual perception is important. Conversely, higher gloss values were observed in BN-added samples. Optimum results were obtained for the hardness parameter with a moderate CNT additive. Consequently, appropriate parameter combinations were suggested for different application scenarios of the sensor structures used in this study. The study's results reveal the effectiveness of ANN in measuring physical parameters and in the advanced modelling and optimisation of such systems.

These biodegradable sensors can be used in areas requiring visual assessment, such as food packaging and environmental humidity and gas measurements. *ΔE* and gloss parameters are critical in colour-based sensing systems. Compared to traditional metal oxide sensors, the advantages of these structures include low cost, biocompatibility, and environmentally friendly production processes. The solution casting technique used in this study is known for its low cost and suitability for industrial production. Furthermore, the widespread availability and processability of the materials used increase the potential for scalable production of these sensors.

Compared with the literature, it was observed that the *ΔE* and gloss values obtained in this study differed depending on the type and ratio of additives. For example, in the studies of CNT-doped biocomposite films by Alam et al. (2022), colour saturation increased while flexibility decreased [21]. The current study observed that the *ΔE* value changed less with low CNT concentrations, which is consistent with the optical stability reported in the literature. On the other hand, the high gloss values of BN-doped sensors are consistent with the findings of researchers such as Giannopoulos and Lima regarding the surface smoothness and optical reflectivity effects of BN [20,47]. In terms of hardness, molecular dynamics simulation studies by Li et al. revealed that the elastic modulus of CNT is higher than that of BN, which explains the broader distribution of hardness values in CNT-doped sensors in our study [28]. Therefore, the results are consistent with experimental perspective and literature on the correlation between material structure and physical properties.

4. CONCLUSIONS

This study presents the evaluation of the results of 4 parameters that have not yet been evaluated together with the production of biodegradable nano-sized BN and CNT doped sensors, which have not been used in other studies in the literature, with three different methods. The study focuses on which type and amount of additives can be preferred for different studies rather than determining a definite additive or concentration. The following conclusions were drawn from this research:

- Our study is one of the first comprehensive comparative studies analysing the physical properties (gloss, ΔE, and hardness) of CNT- and BN-doped biodegradable sensors using ANN (MLP).
- Physical parameters such as ΔE, gloss, and hardness are crucial for sensor performance in visual perception and application conditions.
- The simultaneous measurement and modelling of three physical parameters using an ANN fills a gap in the literature.
- This gap has been filled, particularly in the simultaneous investigation of physical optical parameters with modeling.
- For ΔE, the fifth experimental group with CNT additives should be selected.
- In the glossiness 20° graph, the glossiness is high in BN-doped sensors.
- ΔE is classified with a 95% accuracy rate with MLP.
- Glossiness 20° is classified with 88.3% accuracy, while this value is 84% at glossiness 60°.
- Hardness values are classified with 99.9% accuracy in these sensors.
- For ΔE parameter, 6 ml of water and 0.225 g of glycerol are effective parameters.
- While 9 ml of water and 0.06 g of doped amount are effective parameters for 20° gloss, this is 0.06 g of additive for 60° gloss.
- Regarding hardness, 9 ml of water, 0.225 g of glycerol and 0.06 g of doped amount are effective parameters.
- When the predicted value and the verification experiment results are examined, it is seen that the difference is relatively small.

REFERENCES

[1] W.-Y. Ko, L.-T. Huang, K.-J. Lin, Green technique solvent-free fabrication of silver nanoparticle–carbon nanotube flexible films for wearable sensors, Sens Actuators A Phys 317 (2021) 112437. https://doi.org/10.1016/j.sna.2020.112437.

[2] Y.-T. Lai, J.-C. Kuo, Y.-J. Yang, A novel gas sensor using polymer-dispersed liquid crystal doped with carbon nanotubes, Sens Actuators A Phys 215 (2014) 83–88. https://doi.org/10.1016/j.sna.2013.12.021.

[3] T. Uygunoğlu, B. Şimşek, U. Fidan, Piezoresistive and capacitive cement-based stress sensors designed by incorporating carbon nanotubes doped with graphene nanopowder for structural health monitoring, Sens Actuators A Phys 374 (2024) 115491. https://doi.org/10.1016/j.sna.2024.115491.

[4] M. Ylönen, A. Torkkeli, H. Kattelus, In situ boron-doped LPCVD polysilicon with low tensile stress for MEMS applications, Sens Actuators A Phys 109 (2003) 79–87. https://doi.org/10.1016/j.sna.2003.09.017.

[5] B. Balkanlı, N. Yuksel, M.F. Fellah, Neurotransmitter amino acid adsorption on metal doped boron nitride nanosheets as biosensor: DFT study on neural disease prediagnosis system, Sens Actuators A Phys 366 (2024) 114980. https://doi.org/10.1016/j.sna.2023.114980.

[6] A. Yücel, Ç.V. Yıldırım, AA2024 Alaşımının tornalanmasında nanoakışkan konsantrasyon oranı ve mmy parametrelerinin yüzey pürüzlülüğü ve kesme sıcaklığı üzerindeki etkisi, Manufacturing Technologies and Applications 1 (2020) 18–32.

[7] A. Çakır Şencan, M. Çelik, E.N. Selayet Saraç, Tornalama işleminde uygulanan MMY tekniğinde kullanılan nanoakışkanların işleme performansına etkisi: çevre dostu işleme üzerine bir inceleme, Manufacturing Technologies and Applications 2 (2021) 47–66. https://doi.org/10.52795/mateca.1020081.

[8] N. Kaynak, Fonksiyonel çok katmanlı karbon nanotüpler, Fen Bilimleri Enstitüsü, 2014.

[9] T. Han, A. Nag, S. Chandra Mukhopadhyay, Y. Xu, Carbon nanotubes and its gas-sensing applications: A review, Sens Actuators A Phys 291 (2019) 107–143. https://doi.org/10.1016/j.sna.2019.03.053.

[10] B. Mei, Y. Qin, S. Agbolaghi, A review on supramolecules/nanocomposites based on carbonic precursors and dielectric/conductive polymers and their applications, Materials Science and Engineering: B 269 (2021) 115181. https://doi.org/10.1016/j.mseb.2021.115181.

[11] İ. Topcu, Karbon nanotüp takviyeli alüminyum matriksli almg/knt kompozitlerinin mekanik davranışlarının incelenmesi, Çanakkale Onsekiz Mart Üniversitesi Fen Bilimleri Enstitüsü Dergisi 4 (2018) 99–109. https://doi.org/10.28979/comufbed.359796.

[12] Z. Zhao, K. Teng, N. Li, X. Li, Z. Xu, L. Chen, J. Niu, H. Fu, L. Zhao, Y. Liu, Mechanical, thermal and interfacial performances of carbon fiber reinforced composites flavored by carbon nanotube in matrix/interface, Compos Struct 159 (2017) 761–772. https://doi.org/10.1016/j.compstruct.2016.10.022.
[13] D.C. Ferrier, K.C. Honeychurch, Carbon Nanotube (CNT)-Based Biosensors, Biosensors (Basel) 11 (2021) 486. https://doi.org/10.3390/bios11120486.
[14] S. Rathinavel, K. Priyadharshini, D. Panda, A review on carbon nanotube: An overview of synthesis, properties, functionalization, characterization, and the application, Materials Science and Engineering: B 268 (2021) 115095. https://doi.org/10.1016/j.mseb.2021.115095.
[15] Y. zhang, C. Qin, Y. Wang, J. Cao, Metal clusters modified hexagonal boron nitride for adsorption and sensing of lithium batteries thermal runaway gases, Sens Actuators A Phys 379 (2024) 115929. https://doi.org/10.1016/j.sna.2024.115929.
[16] R. İnan, Nanokompozit tekstil yüzeylerinin iletken hale getirilmesi ve sensör özelliği kazandırılması , Doktora Tezi, Marmara Üniversitesi, 2024.
[17] G.I. Giannopoulos, On the buckling of hexagonal boron nitride nanoribbons via structural mechanics, Superlattices Microstruct 115 (2018) 1–9. https://doi.org/10.1016/j.spmi.2018.01.016.
[18] Y. Göncü, M. Geçgin, F. Bakan, N. Ay, Electrophoretic deposition of hydroxyapatite-hexagonal boron nitride composite coatings on Ti substrate, Materials Science and Engineering: C 79 (2017) 343–353. https://doi.org/10.1016/j.msec.2017.05.023.
[19] T. Han, F. Scarpa, N.L. Allan, Super stretchable hexagonal boron nitride Kirigami, Thin Solid Films 632 (2017) 35–43. https://doi.org/10.1016/j.tsf.2017.03.059.
[20] D.M. Lima, A.C. Chinellato, M. Champeau, Boron nitride-based nanocomposite hydrogels: preparation, properties and applications, Soft Matter 17 (2021) 4475–4488. https://doi.org/10.1039/D1SM00212K.
[21] R.B. Alam, Md.H. Ahmad, M.R. Islam, Effect of MWCNT nanofiller on the dielectric performance of bio-inspired gelatin-based nanocomposites, RSC Adv 12 (2022) 14686–14697. https://doi.org/10.1039/D2RA01508K.
[22] R.B. Alam, Md.H. Ahmad, M.R. Islam, Bio-inspired gelatin/single-walled carbon nanotube nanocomposite for transient electrochemical energy storage: An approach towards eco-friendly and sustainable energy system, Heliyon 7 (2021) e07468. https://doi.org/10.1016/j.heliyon.2021.e07468.
[23] S. Sankaran, K. Deshmukh, M.B. Ahamed, K.K. Sadasivuni, M. Faisal, S.K.K. Pasha, Electrical and Electromagnetic Interference (EMI) shielding properties of hexagonal boron nitride nanoparticles reinforced polyvinylidene fluoride nanocomposite films, Polymer-Plastics Technology and Materials 58 (2019) 1191–1209. https://doi.org/10.1080/03602559.2018.1542725.
[24] S.O. Akinnawo, Advance nanocomposites from biopolymers and fillers: sources, characterization, and end-use applications, Polymer-Plastics Technology and Materials 63 (2024) 570–604. https://doi.org/10.1080/25740881.2023.2296659.
[25] H. Gergeroglu, S. Yildirim, M.F. Ebeoglugil, Nano-carbons in biosensor applications: an overview of carbon nanotubes (CNTs) and fullerenes (C60), SN Appl Sci 2 (2020) 603. https://doi.org/10.1007/s42452-020-2404-1.
[26] M. Emanet, Ö. Sen, I.Ç. Taşkin, M. Çulha, Synthesis, functionalization, and bioapplications of two-dimensional boron nitride nanomaterials, Front Bioeng Biotechnol 7 (2019) 363. https://doi.org/10.3389/fbioe.2019.00363.
[27] Y. Li, Z. Han, D. Wang, M. Tao, Preparation of hexagonal boron nitride nanosheets in low eutectic solvent and its application for dye adsorption, Colloids Surf A Physicochem Eng Asp 700 (2024) 134813. https://doi.org/10.1016/j.colsurfa.2024.134813.
[28] T. Li, Z. Tang, Z. Huang, J. Yu, A comparison between the mechanical and thermal properties of single-walled carbon nanotubes and boron nitride nanotubes, Physica E Low Dimens Syst Nanostruct 85 (2017) 137–142. https://doi.org/10.1016/j.physe.2016.08.012.
[29] L. Algharagholy, T. Pope, Q. Al-Galiby, H. Sadeghi, S.W.D. Bailey, C.J. Lambert, Sensing single molecules with carbon–boron-nitride nanotubes, J Mater Chem C Mater 3 (2015) 10273–10276. https://doi.org/10.1039/C5TC02284C.
[30] Y. Zhan, E. Lago, C. Santillo, A.E. Del Río Castillo, S. Hao, G.G. Buonocore, Z. Chen, H. Xia, M. Lavorgna, F. Bonaccorso, An anisotropic layer-by-layer carbon nanotube/boron nitride/rubber composite and its application in electromagnetic shielding, Nanoscale 12 (2020) 7782–7791. https://doi.org/10.1039/C9NR10672C.
[31] C. Yuan, A. Tony, R. Yin, K. Wang, W. Zhang, Tactile and thermal sensors built from carbon–polymer nanocomposites—A Critical Review, Sensors 21 (2021) 1234. https://doi.org/10.3390/s21041234.
[32] V.D.N. Bezzon, T.L.A. Montanheiro, B.R.C. de Menezes, R.G. Ribas, V.A.N. Righetti, K.F. Rodrigues, G.P. Thim, Carbon nanostructure-based sensors: A brief review on recent advances, Advances in Materials Science and Engineering 2019 (2019) 1–21. https://doi.org/10.1155/2019/4293073.
[33] N. Boroznina, I. Zaporotskova, S. Boroznin, L. Kozhitov, P. Zaporotskov, Comparative analysis of sensory activity of carbon and boron nitride nanotubes with boundary modification, International Journal of Theoretical and Applied Nanotechnology 8 (2020) 21–28. https://doi.org/10.11159/ijtan.2020.004.
[34] I.M. Patil, M. Lokanathan, B. Ganesan, A. Swami, B. Kakade, Carbon nanotube/boron nitride nanocomposite as a significant bifunctional electrocatalyst for oxygen reduction and oxygen evolution reactions, Chemistry – A European Journal 23 (2017) 676–683. https://doi.org/10.1002/chem.201604231.

[35] S.K. Vashist, D. Zheng, K. Al-Rubeaan, J.H.T. Luong, F.-S. Sheu, Advances in carbon nanotube based electrochemical sensors for bioanalytical applications, Biotechnol Adv 29 (2011) 169–188. https://doi.org/10.1016/j.biotechadv.2010.10.002.
[36] P. Bahrami Miyanji, D. Semnani, A. Hossein Ravandi, S. Karbasi, A. Fakhrali, S. Mohammadi, Fabrication and characterization of chitosan-gelatin/single-walled carbon nanotubes electrospun composite scaffolds for cartilage tissue engineering applications, Polym Adv Technol 33 (2022) 81–95. https://doi.org/10.1002/pat.5492.
[37] R.B. Alam, Md.H. Ahmad, S.F.U. Farhad, M.R. Islam, Significantly improved dielectric performance of bio-inspired gelatin/single-walled carbon nanotube nanocomposite, J Appl Phys (2022) 131. https://doi.org/10.1063/5.0077896.
[38] R.B. Alam, Md.H. Ahmad, S.M.N. Sakib Pias, E. Mahmud, M.R. Islam, Improved optical, electrical, and thermal properties of bio-inspired gelatin/SWCNT composite, AIP Adv (2022) 12. https://doi.org/10.1063/5.0089118.
[39] Z. Yang, S. Chaieb, Y. Hemar, Gelatin-Based Nanocomposites: A Review, Polymer Reviews 61 (2021) 765–813. https://doi.org/10.1080/15583724.2021.1897995.
[40] J. Hassan, S. Naz, A. Haider, A. Raza, A. Ul-Hamid, U. Qumar, J. Haider, S. Goumri-Said, M.B. Kanoun, M. Ikram, h-BN nanosheets doped with transition metals for environmental remediation; a DFT approach and molecular docking analysis, Materials Science and Engineering: B 272 (2021) 115365. https://doi.org/10.1016/j.mseb.2021.115365.
[41] S. Vairagade, N. Kumar, R.P. Singh, Recent advancements and applications in thermally conductive polymer nanocomposites, Polymer-Plastics Technology and Materials 63 (2024) 1371–1420. https://doi.org/10.1080/25740881.2024.2330699.
[42] C. Söğütlü, A. Sönmez, Değişik koruyucular ile işlem görmüş bazı yerli ağaçlarda UV ışınlarının renk değiştirici etkisi, Gazi Üniversitesi Mühendislik Mimarlık Fakültesi Dergisi 21 (2013) 151–160.
[43] C. Kumah, N. Zhang, R.K. Raji, R. Pan, Color Measurement of Segmented Printed Fabric Patterns in Lab Color Space from RGB Digital Images, Journal of Textile Science and Technology 05 (2019) 1–18. https://doi.org/10.4236/jtst.2019.51001.
[44] F. Tarlak, M. Özdemir, M. Melikoğlu, Computer vision system approach in colour measurements of foods: Part II. validation of methodology with real foods, Food Science and Technology 36 (2016) 499–504. https://doi.org/10.1590/1678-457X.02616.
[45] P.J. Baldevbhai, Color Image Segmentation for Medical Images using L*a*b* Color Space, IOSR Journal of Electronics and Communication Engineering 1 (2012) 24–45. https://doi.org/10.9790/2834-0122445.
[46] N. Fdhal, M. Kyan, D. Androutsos, A. Sharma, Color Space Transformation from RGB to CIELAB Using Neural Networks, in: Advances in Multimedia Information Processing - PCM 2009, 2009: pp. 1011–1017. https://doi.org/10.1007/978-3-642-10467-1_97.
[47] G.I. Giannopoulos, On the buckling of hexagonal boron nitride nanoribbons via structural mechanics, Superlattices Microstruct 115 (2018) 1–9. https://doi.org/10.1016/j.spmi.2018.01.016.